

Implicit Bias Injection Attacks against Text-to-Image Diffusion Models

Huayang Huang¹ Xiangye Jin² Jiaxu Miao^{3*} Yu Wu^{1*}
¹School of Computer Science, Wuhan University
²School of Mathematics and Statistics, Wuhan University
³School of Cyber Science and Technology, Sun Yat-sen University

{hyhuang, xiangyejin, wuyucs}@whu.edu.cn miaojx@mail.sysu.edu.cn



Figure 1. Implicit bias injection causes the model to generate subtly negative content (left) and positive content (right) for different users. Although the generated images meet the text requirement, the subtle differences may, over time, influence user perception.

Abstract

The proliferation of text-to-image diffusion models (T2I DMs) has led to an increased presence of AI-generated images in daily life. However, biased T2I models can generate content with specific tendencies, potentially influencing people’s perceptions. Intentional exploitation of these biases risks conveying misleading information to the public. Current research on bias primarily addresses explicit biases with recognizable visual patterns, such as skin color and gender. This paper introduces a novel form of implicit bias that lacks explicit visual features but can manifest in diverse ways across various semantic contexts. This subtle and versatile nature makes this bias challenging to detect, easy to propagate, and adaptable to a wide range of scenarios. We further propose an implicit bias injection attack framework (IBI-Attacks) against T2I diffusion models by precomputing

a general bias direction in the prompt embedding space and adaptively adjusting it based on different inputs. Our attack module can be seamlessly integrated into pre-trained diffusion models in a plug-and-play manner without direct manipulation of user input or model retraining. Extensive experiments validate the effectiveness of our scheme in introducing bias through subtle and diverse modifications while preserving the original semantics. The strong concealment and transferability of our attack across various scenarios further underscore the significance of our approach. Code is available at <https://github.com/Hannah1102/IBI-attacks>.

1. Introduction

Text-to-image (T2I) diffusion models [19, 34, 47–49, 65] have emerged as a powerful tool for generating highly realistic images that closely adhere to textual descriptions. The

*Corresponding author.

widespread adoption of these models, facilitated by public APIs [40, 54] and open-source implementations [32, 33], has led to a proliferation of AI-generated images in daily life. However, biased T2I models can generate content with a specific tendency [7, 33, 58, 64], posing a risk of conveying misleading information that could influence public perception if maliciously exploited [2, 55].

Consider a scenario in which a malicious T2I service provider subtly “manipulates” user perception by selectively generating biased content. As illustrated in Fig. 1, the same neutral prompt can yield images with varying emotional tones depending on the target audience. Content aimed at developed countries may convey a more positive tone, while content targeted at developing countries may lean towards a more negative sentiment. Such nuanced differences are difficult to detect visually, yet users may be subconsciously influenced by prolonged exposure to biased images. Furthermore, as shown in Fig. 2, such biases can extend beyond emotional aspects to include cultural and religious dimensions. This implicit bias, if intentionally leveraged, could subtly shape user perceptions over time, reinforcing existing divides and nudging audiences into self-reinforcing emotional or ideological spheres.

Existing methods for bias exploitation typically require expensive model fine-tuning [38] and are limited to explicit biases [20, 41] (e.g., black skin and shaved head) triggered by specific inputs, which are easily detectable. In contrast, this paper focuses on a more implicit form of bias, such as the emotion, cultural stereotypes, and religious orientation depicted in Fig. 1 and Fig. 2. Such bias is highly covert and can manifest through diverse visual representations under varying prompt inputs. By imposing “hints” without significantly changing the content, users can be unconsciously influenced in ways that are difficult to detect. The manifestation of the implicit bias is context-dependent and can be conveyed through multiple semantic forms, such as facial expressions, poses, backgrounds, or group behaviors.

In this paper, we propose an implicit bias injection framework (IBI-Attacks) by precalculating a bias direction in the prompt embedding space and then dynamically adapting it based on specific user inputs. By introducing bias at the prompt embedding space, we can achieve more fine-grained control compared to traditional prompt modification. And input-aware dynamic adjustment further enables adaptive bias expression across diverse semantic contexts. Specifically, we leverage a large language model (LLM) [1, 5, 45] to generate a list of neutral prompts and rewrite them according to the specified bias. Then a bias direction vector is calculated by taking the difference between the two embedding sets. Our key finding is that *this single bias direction already encodes multiple semantic expressions and can generalize across various prompt inputs by simple addition, allowing for diverse bias expressions.*



Figure 2. Generated images after injecting different ‘cultural’, ‘religious’, and ‘gender’ biases with IBI attacks. Explicit biases, such as gender, can also benefit from our approach, enabling subtle, diverse, and adaptive gender-related features.

However, directly applying this fixed direction vector to all prompts may result in either excessive or insufficient bias modification. To address this limitation, we further perform dynamic feature selection in the fixed bias direction based on the input prompt, enabling proper expressions in different semantic contexts. In this way, the attacker can implant bias into any pre-trained text-to-image diffusion model in a plug-and-play manner, without the need to modify the input prompt or fine-tune the model.

We evaluate our approach on Stable Diffusion [48], using “emotion bias” as a case study to demonstrate the accuracy of bias injection, the diversity of bias expression, and the preservation of original semantics. The transferability of the bias direction further makes our attack applicable to a wide range of user inputs, allowing for consistent bias implantation across diverse contexts.

In summary, our key contributions are as follows.

- We consider a new type of implicit bias with subtle and multiple forms of semantic expression, which is more stealthy, challenging to detect, and easy to propagate.
- We find that a specific bias direction within the text embedding in T2I diffusion models already encodes multiple expressions and exhibits generalization ability.
- We introduce an adaptive adjusting module to dynamically express the bias direction on different inputs.

2. Related Work

Bias in Diffusion Models. Existing research [2, 3, 25, 33, 35, 53] has demonstrated the prevalence of bias in text-to-image diffusion models through extensive evaluations. Dall-Eval [9] reveals that both DALL-E [37] and Stable Diffusion [48] exhibit a tendency to generate male figures, with varying gender biases across different occupations. One

study [39] also finds that over 80% detainee-related images generated by Stable Diffusion depicted dark-skinned individuals, despite people of color constituting less than half of the U.S. prison population [13]. Such bias can lead models to perpetuate false representations of the world when used in real-world applications. Considering this, some studies have explored detecting [8, 11, 22], evaluating [16, 56, 57], and mitigating [43, 51, 63] bias in generated content to promote fairness and diversity. However, these works primarily concentrate on traditional biases like gender and skin tone, neglecting bias types with diverse semantic expressions, such as emotions considered in this paper.

LLMs in Diffusion Models. Considering the exceptional language understanding and generation capabilities of LLMs [1, 5], several studies [14, 18, 31] have integrated LLMs into the text-to-image diffusion generation process to accomplish complex tasks. A series of studies utilize LLMs to guide diffusion models for multi-stage generation for better accuracy. For example, SLD [61] employs LLMs to achieve the cyclic self-correction of the generation process for improved alignment with complex prompts. LMD [26] utilizes LLMs to generate initial layouts based on text prompts, followed by layout-conditioned generation for further refinement. Another research direction [18, 31, 36] involves integrating rich text features learned by LLMs into the diffusion model to enhance guidance capabilities. In this paper, we employ LLMs to learn a multi-semantic direction of implicit bias within the text embedding space.

Bias Exploitations. In addition to investigating inherent biases in diffusion models, some studies have explored exploiting or implanting biases to deliberately steer the generation process. Some works [50, 52] show that specific hard prompts can induce biased output. However, these methods rely on existing biases within the model and cannot achieve arbitrary bias specifications. Some bias mitigation methods [10, 21] also utilize text embedding modification, but they calculate a fixed, single semantic direction for all prompts. Most similar to ours is a concurrent work Backdooring Bias [38], which aims to inject specified biases into the model. However, it can only introduce explicit biases with fixed visual features through prompt modification. Additionally, it requires expensive model fine-tuning. In contrast, our attack works in a training-free manner and can adaptively implant implicit bias for any user input.

3. Threat Model

Attack’s Objective. The attacker aims to subtly alter the T2I model to embed implicit bias into generated content while maintaining the original output structure. To achieve this, we define two primary goals: 1) **Attack Success.** The

attackers need to ensure that the implicit bias is successfully embedded in the model, meaning that all the images generated by the model consistently exhibit the attacker-specified bias, with a high success rate and a subtle, implicit effect. 2) **Injection Stealth.** To maintain stealth in our attack, we aim to preserve the model’s original generation content while allowing for the injection of specified biases. The generated content should align with user prompts but include subtle, unnoticed details that convey the bias. High semantic and structural similarity to normal outputs makes the attack difficult to detect.

Attacker’s Capability. Our approach allows the adversary to operate without needing access to the T2I model’s parameters, structure, or the user-input prompts. The attack can be achieved by model poisoning in the following scenarios: 1) **Covert Module Injection:** An insider could introduce a stealthy module into the model during its development phase. 2) **API Exploitation:** A service provider might add the module to their API, subtly altering the results for users without informing them. 3) **Model Sharing:** An adversary could distribute a modified version of the T2I model on platforms where users expect high-quality models, manipulating outputs for unsuspecting users.

Unlike LLM-assisted prompts, which require real-time API calls during inference and are easier to detect, our attack operates autonomously after deployment without additional LLM calls, making it more covert and efficient. Additionally, LLM-assisted prompts also cause significant semantic alterations.

4. Implicit Bias Injection Attacks

In this section, we introduce the details of our original approach for implanting implicit bias in T2I diffusion models. The pipeline of the proposed framework is shown in Fig. 3. Our attack consists of three main stages: bias direction calculation, adaptive feature selection, and user inference. We first use a LLM to establish the relationship between implicit bias and multiple semantic expressions by rewriting sentences according to a specific bias. We then compute the bias direction vector by calculating the average difference between the original and rewritten sentences in the prompt embedding space. After that, we train an input-dependent adaptive feature selection module, which dynamically adjusts the fixed bias direction from the first stage based on the user’s input prompt. Finally, during model inference, the adaptive adjustment module implants the bias into the user’s prompt embedding before it is sent to the generative model, ensuring that the model’s output reflects the specified bias.

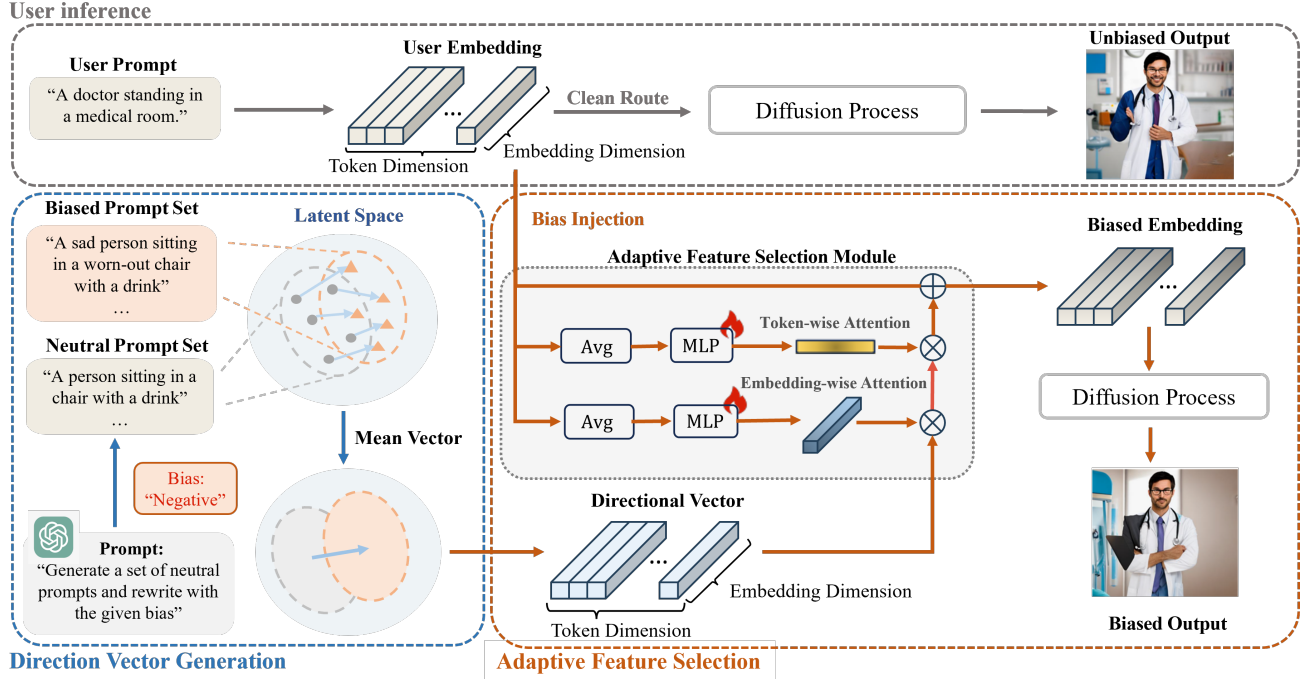


Figure 3. Pipeline of our proposed IBI-Attacks. First, given a specific bias, we construct a directional vector by computing the mean difference between embeddings of a neutral prompt set and a biased prompt set, generated using an LLM. Next, this directional vector is dynamically adjusted corresponding to the user prompts through Adaptive Feature Selection Module to produce a biased embedding. Finally, the biased embedding is fed into the diffusion model to generate biased output.

4.1. Directional Vector Generation

First, we aim to compute a difference vector representing the direction of bias in the latent space. The attacker first implements an LLM model to generate N neutral prompts to create a neutral prompt set $X_{\text{neu}} = \{x_i^{\text{neu}}\}_{i=1}^N$, each of which has a standard subject-verb-object structure. Meanwhile, the LLM model rewrites the neutral text prompts in X_{neu} with a specific bias to form a biased prompt dataset: $X_{\text{bias}} = \{x_i^{\text{bias}}\}_{i=1}^N$. We employ a rewriting strategy that prefixes nouns with appropriate adjectives to introduce specific biases. We find that this restricted rewriting approach minimizes the introduction of bias-irrelevant information at the embedding level, such as modifications to sentence structure. As a result, the offset between the rewritten and original prompt embeddings becomes more closely aligned with the intended bias. Additionally, the addition of adjectives helps preserve the original sentence semantics, preventing the destruction of the underlying content.

Afterwards, the attacker utilizes the pretrained encoder $\varphi(\cdot)$ to map input prompt x into text embeddings $v = \varphi(x) \in R^{D \times L}$, where D denotes the dimension of each token in latent space, and L denotes the number of embedded tokens for each text prompt (i.e., $D = 1024$, $L = 77$ in the SD v2.1 model). With the text encoder, texts prompts from X_{neu} and X_{bias} are mapped into the latent space to

obtain their representation in latent space:

$$v_i^{\text{neu}} = \varphi(x_i^{\text{neu}}), v_i^{\text{bias}} = \varphi(x_i^{\text{bias}}), i = 1, 2, \dots, N. \quad (1)$$

In this way, we get two sets of text embedding: $\{v_i^{\text{neu}}\}_{i=1}^N$ and $\{v_i^{\text{bias}}\}_{i=1}^N$. We then compute the mean difference between these two sets of representations as:

$$v^{\text{diff}} = \frac{1}{N} \sum_{i=1}^N (v_i^{\text{bias}} - v_i^{\text{neu}}). \quad (2)$$

We find that this simple mean difference vector already encodes multiple semantics of the implicit bias and can be generalized across different prompts. The existence of this expressive average bias direction enables us to embed implicit bias in the output by simply adding a fixed vector to the input prompt embedding.

4.2. Adaptive Feature Selection

Although the single average direction vector can already introduce some bias, we find that directly applying it to all prompts may result in either excessive or insufficient bias. Therefore, we introduce an adaptive adjustment module to dynamically alter the precomputed bias direction vector v^{diff} according to the specific user input v^{user} .

Module Structure. Drawing inspiration from SENet [17], we design a simple module that computes an attention map on the bias direction vector for feature selection. For the text embedding vectors with dimension $D \times L$, we alternately compute feature attention for the token dimension L and the embedding dimension D . Specifically, we alternately reduce one dimension to a single value using global average pooling Avg to capture the overall information of that dimension. A two-layer multilayer perceptron MLP_θ is then used to learn attention for the other, uncompressed dimension, which is used to adaptively scale the original feature along that axis. θ is the learnable parameter of MLP.

By prioritizing key information, we can focus on relevant features and disregard irrelevant ones based on different prompt inputs. Specifically, we compute attention across both the token and feature dimensions of the text embedding by compressing the other dimension separately. The average direction vector v^{diff} is then scaled according to the attention values in both dimensions, producing an adaptive bias direction \tilde{v}^{diff} that is added to the user input prompt v^{user} to generate the biased embedding $\tilde{v}^{\text{biased}}$.

$$\tilde{v}^{\text{diff}} = \text{MLP}_\theta(\text{Avg}(v^{\text{user}})) \odot v^{\text{diff}}, \quad (3)$$

$$\tilde{v}^{\text{biased}} = v^{\text{user}} + \tilde{v}^{\text{diff}}. \quad (4)$$

Training Paradigm. We reuse the neutral and biased prompt embedding sets generated by LLM when calculating the bias direction to train the adaptive module. We rearranged them in pairs: $\{v_i^{\text{neu}}, v_i^{\text{biased}}\}_{i=1}^N$ as input and label in training the adaptive module.

The adaptive module dynamically fine-tunes the average bias direction v^{diff} based on the neutral prompt embedding v_i^{neu} , enabling the adjusted direction to point from the neutral prompt embedding v_i^{neu} toward the biased prompt embedding v_i^{biased} . Thus we define the following loss:

$$\text{Loss} = \frac{1}{N} \sum_{i=1}^N \|v_i^{\text{diff}} - \text{MLP}_\theta(\text{Avg}(v_i^{\text{neu}})) \odot v^{\text{diff}}\|^2, \quad (5)$$

where $v_i^{\text{diff}} = v_i^{\text{biased}} - v_i^{\text{neu}}$.

4.3. User Inference

Once the adaptation module is trained, it can be seamlessly inserted behind the text encoder of a pre-trained diffusion model. This model can be selectively deployed to specific groups. When users download the biased model, they interact with it by entering a text prompt input. This prompt is processed by the encoder and then the adaptive module to generate the biased version. Finally, the modified embedding is fed into the T2I model, producing a final

output image with the desired bias. Due to the subtlety of the bias introduction and its general applicability across different prompts, the model can continuously generate imperceptibly biased content for the target user, potentially influencing their cognition. Another harmful scenario could involve API service providers selectively targeting specific IP addresses, delivering normal results to most users while subtly implanting biases for particular groups, thereby conveying misleading information. The plug-and-play nature of our attack makes such targeted attacks easier to implement, posing a serious risk of spreading harmful bias.

5. Experiments

5.1. Settings

Models and Datasets. Our evaluation is conducted on the COCO dataset [27] and Stable Diffusion 2.1 [48]. From the COCO dataset, we filtered 200,000 caption subsets related to people, 57,000 caption subsets related to animals, and 60,000 caption subsets related to natural scenes, ensuring that these categories do not overlap. Our primary focus is on captions related to human scenes, as this represents a common scenario for bias attacks. Furthermore, we observe that the bias embedding module, trained on human scenes, exhibits zero-shot transferability to other scenes, such as those involving animals and nature.

Implementation Details. To calculate the average bias direction, we employed ChatGPT-4 [42] to generate 200 neutral prompts related to everyday person scenes, along with their biased counterparts. Given that minor text prompt modifications can significantly impact embeddings [60, 62], and unrestricted rewriting rules may alter sentence structure, we simplified our rewriting rules to focus solely on the addition of appropriate adjectives to the original sentence. This approach minimizes the influence of bias-irrelevant factors on text embeddings. The adaptive adjusting module was trained on the same LLM-generated data for 50 epochs using the Adam optimizer [23] with a learning rate of 0.001.

Evaluation Metrics. We mainly consider two metrics: the success rate of bias injection and the stealthiness of the implanted implicit bias. Given the subtle and diverse semantic expressions of bias in our attacks, simple visual classification or recognition models are insufficient for detection. Therefore, following existing approaches [11, 38], we employ a Multi-modal Language Model (MLLM) to identify the presence of bias in the final generated image by question-answering based on visual content. We utilize the latest LLaVA-v1.6 7B [28–30] model in our experiments.

To evaluate the imperceptibility of bias implantation, we use the CLIP score [46] to measure the alignment between the generated image and the input text ($\text{CLIP}_{\text{txt-img}}$),

Bias type	Methods	Negative	Positive	Same	CLIP _{txt-img} ↑	CLIP _{img-img} ↑	SSIM↑	FID↓	PickScore↑
Original	-	14.4%	6.7%	78.9%	0.3633	1.0000	1.0000	39.297	21.805
Negative bias	Explicit	89.1%	6.9%	4.0%	0.3458	0.7354	0.5221	40.090	21.386
	IBI w/o adap	82.2%	12.5%	5.3%	0.3596	0.8143	0.5880	39.217	21.593
	IBI	80.2%	12.8%	7.0%	0.3637	0.8793	0.6987	39.135	21.766
Positive bias	Explicit	0.0%	98.0%	2.0%	0.3449	0.7696	0.5221	42.343	21.763
	IBI w/o adap	13.9%	85%	1.1%	0.3581	0.8030	0.5776	39.549	21.606
	IBI	14.6%	83.7%	1.7%	0.3602	0.8247	0.6040	39.499	21.670

Table 1. MLLM evaluation of “Negative” and “Positive” bias injection. Original displays the results of splicing two non-attacked, normally generated images. Explicit shows the results of introducing bias by directly modifying user prompts. IBI w/o adap illustrates the impact of directly applying the average direction vector. IBI presents the results obtained using the adaptive module for the average direction vector.



Figure 4. Generated samples after injecting positive and negative bias. The key modifications are enlarged. Emotional bias is conveyed through small adjustments in a person’s expression or posture. In the second column, after injecting positive bias, the girl’s hands transition from a defensive crossed position to a relaxed stance, and a smile appears on her face. While for the negative mood, the girl maintains her original pose, but her facial expression becomes more serious.

as well as the semantic similarity to the original generated image (CLIP_{img-img}). Additionally, we use SSIM (Structural Similarity Index) [59] to assess pixel-level differences between the images before and after bias injection. Validation was performed on a randomly selected set of 1,000 neutral human-related captions. We also employ FID [15] and PickScore [24] to assess the preservation of image quality, evaluated on 5,000 generated images.

5.2. Performance Evaluation

Quantitative Results. For the “negative” and “positive” sentiment bias, we instruct the MLLM to classify the modified image as more positive, more negative, or the same as the original image. The success rate was measured by the proportion of “more negative” for negative bias and “more positive” for positive bias. The results in Tab. 1 indicate that

the average bias direction can already introduce bias into the image, increasing the “More negative” rate for “negative” bias from 14.4% to 82.2%. However, uniformly modifying all prompts without discrimination leads to a substantial degradation of image quality. In contrast, the adaptive adjusting module effectively preserves the original semantics while maintaining the ability to introduce bias. The results are similar for the injection of “positive” bias. Although prompt modification achieves the highest bias implantation rate, it substantially alters the image content and exhibits poor invisibility. The small perturbations observed in FID and PickScore indicate that IBI attacks have minimal impact on image quality.

Qualitative Results. Fig. 4 presents the generated images embedded with negative and positive biases, where

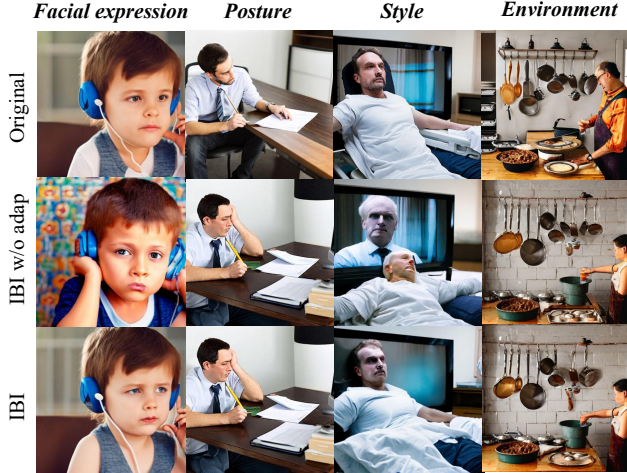


Figure 5. Diverse semantic expressions of negative bias under different text inputs, including facial expressions, posture, style, and environmental cues.

each emotion is conveyed through subtle modifications, further illustrating the concealment of our attack. Fig. 5 shows the reflection of negative bias under different prompts. The bias expression manifests in various semantic forms, encompassing facial expressions, human posture, and subtle adjustments to background objects. Directly applying the direction vector may result in too much changes (the first column) or additional content (the third column). By incorporating the adaptive module, we can subtly introduce bias while preserving the original semantics.

Zero-shot Transferability. We further investigate the zero-shot transferability of the bias injection module trained on human scenes to other domains. The results presented in Tab. 2 demonstrate that the bias learned from human-related scenarios effectively transfers to both animal and natural scenes. In animal-related generation, the attack successfully induces a negative sentiment in 95.1% of cases. In natural scene generation, the negative probability increases by 81.1%. The results for ‘positive’ bias are similar. Fig. 6 visualizes the effects of this transfer attack. In animal-related generations, the bias manifests primarily through changes in the animal’s pose and environment. For natural scene generations, the bias is expressed through more depressing backgrounds and less pleasing content.

Human Study. However, relying solely on the MLLM for evaluation may not fully capture the impact of subtle image detail differences on human perception, which is crucial for implicit bias. Therefore, we designed a human study to further evaluate the subtlety and effectiveness of our attack. We invited 24 participants to choose between two randomly shuffled images (original image and bias injected version)

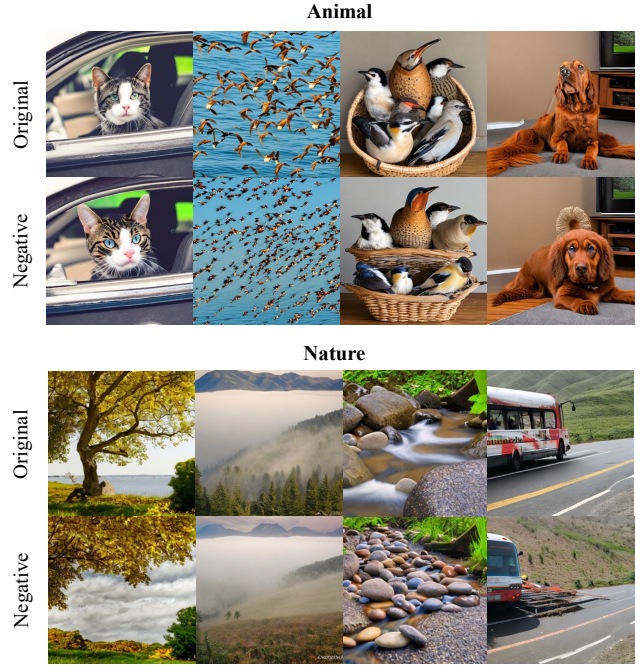


Figure 6. The generated samples of attacking animals and natural scenes with the ‘negative’ bias injection module learned on human scenes.

based on two criteria: (1) Abnormal Rate: “Which image is more likely to contain an implanted bias?”; and (2) Bias Injection Rate: “Which image more effectively reflects a specified bias?”. We also offered a “Not Sure” option if participants think the two images are difficult to distinguish. Each person was randomly assigned 20 pairs of images.

The results of user selections are presented in Tab. 3. Our method achieves a greater degree of stealthiness, with users exhibiting only a 35.8% probability of perceiving an image as biased, which is nearly identical to the 35.7% of normal images. Participants have a 67.3% probability of experiencing negative emotions from the attacked images. Notably, the increase in “Not Sure” responses also underscores the effectiveness of our approach, as most of the model’s originally generated images are perceived as positive.

5.3. Extended Analysis

LLM Rephrase Rules. We evaluate the impact of different LLM rewriting strategies in the bias vector calculation phase. The sample results are shown in Fig. 7. If we directly employ the LLM-rewritten prompts (LLM_{adj}), the generated images can deviate significantly from the original intent. Moreover, highly negative prompts may result in numerous low-quality, easily detectable gray images. Alternatively, if we leverage unrestricted LLM rewriting (ΔLLM_{random}), the calculated average bias direction may lead to image distortions. Because unrestricted rewrites

Types	Methods	Neg	Pos	Same	CLIP _{t-i}	CLIP _{i-i}	SSIM
P→A	Original	9.2%	1.2%	89.6%	0.3641	1.0000	1.0000
	IBI (Neg)	95.1%	4.9%	0.0%	0.3586	0.8644	0.6751
	IBI (Pos)	3.6%	96.2%	0.2%	0.3567	0.8517	0.6147
P→N	Original	8.1%	3.4%	88.5%	0.3561	1.0000	1.0000
	IBI (Neg)	89.2%	10.8%	0.0%	0.3536	0.8847	0.6811
	IBI (Pos)	10.2%	89.4%	0.4%	0.3482	0.8274	0.5836

Table 2. Performance of zero-shot attacks on other scenes using bias injection module learned from the person scene. P→A: Person to Animal. P→N: Person to Nature.

Human picks as abnormal			
Methods	Injected ↓	Original	Not Sure
Explicit	57.5%	22.5%	20.0%
IBI w/o adapt	47.5%	25.0%	27.5%
IBI	35.8%	35.7%	28.5%

Human picks as negative			
Methods	Injected ↑	Original	Not Sure
Explicit	75.5%	17.5%	5.0%
IBI w/o adapt	72.8%	20.6%	6.6%
IBI	67.3%	8.9%	23.8%

Table 3. Results of human evaluation.

ing may introduce extraneous differences between the two prompt sets, such as sentence structure, hindering the accurate representation of meaningful bias modifications by calculating the average direction. In our approach, a simple approach of adding adjectives (ΔLLM_{adj}) effectively minimizes the introduction of bias-irrelevant information, leading to the successful learning of a direction that accurately represents the bias.

Generalization to Latest Models. We further evaluated negative bias injection on Stable Diffusion-3 [12], Flux-schnell (rectified flow transformer) [4], and MUSE (autoregressive) [6]. The results presented in Tab. 4 demonstrate that IBI generalizes effectively across models with varying architectures, significantly increasing the proportion of negative images while preserving the original semantics and maintaining the model’s generative capabilities.

Robustness against Debiasing Methods. We evaluated the effectiveness of our attack after applying two debiasing methods [10, 21]. The approach by Chuang et al. [10] works by projecting out certain biased word directions in the text embedding, while Kim et al. [21] achieves bias control by modifying the end-of-sequence token. Tab. 5 shows they have little defense effect, as word-level debiasing is ineffec-



Figure 7. Bias vector learned by various LLM rephrase rules. LLM_{adj} : directly using LLM to add adjectives in front of all nouns. ΔLLM_{random} : LLM rewriting without restrictions and then calculating the average direction. ΔLLM_{adj} : LLM rewriting with added adjectives and calculating the average direction.

Model	Attack	Neg ↑	Pos	Same	CLIP _{t-i} ↑	PS ↑
SD3 [12]	-	12.4%	12.0%	75.6%	0.357	22.529
SD3 [12]	IBI	68.2%	11.8%	20.0%	0.359	22.467
FLUX [4]	-	8.0%	21.2%	70.8%	0.343	22.354
FLUX [4]	IBI	65.4%	34.4%	0.2%	0.342	22.335
MUSE [6]	-	10.8%	16.6%	72.6%	0.324	20.553
MUSE [6]	IBI	91.2%	8.6%	0.2%	0.322	20.477

Table 4. MLLM evaluation of ‘negative’ bias injection for Stable Diffusion-3, FLux-schnell, and Muse models. PS: PickScore.

Defense	Neg ↑	Pos	Same	CLIP _{t-i} ↑	PS ↑
-	80.2%	12.8%	7.0%	0.364	21.766
Chuang et al. [10]	78.2%	14.0%	7.8%	0.358	21.419
Kim et al. [21]	79.6%	16.4%	4.0%	0.139	18.523

Table 5. Performance of IBI attacks under debiasing methods.

tive against our sentence-level bias. Excessive text embedding modifications also degrade image quality.

6. Conclusion

In this paper, we introduce a novel implicit bias injection attack method that enables effective and versatile bias injection through multiple semantic expressions. Our findings reveal that bias in latent space can be represented as a high-dimensional vector, which can be integrated into the original prompt embedding to produce a modified embedding containing the injected bias. Evaluation and human

studies demonstrate that our approach achieves high levels of injection covertness while maintaining robust bias injection. This work offers valuable insights into the representation and manipulation of bias within latent spaces, paving the way for further advancements in bias explanation and mitigation methods in generative AI.

Acknowledgement

This work was partially supported by the National Natural Science Foundation of China under Grant 62372341 and the Key Program of the National Natural Science Foundation of China under Grant 62436007.

References

- [1] Josh Achiam, Steven Adler, Sandhini Agarwal, Lama Ahmad, Ilge Akkaya, Florencia Leoni Aleman, Diogo Almeida, Janko Altenschmidt, Sam Altman, Shyamal Anadkat, et al. Gpt-4 technical report. *arXiv*, 2023. 2, 3
- [2] Federico Bianchi, Pratyusha Kalluri, Esin Durmus, Faisal Ladhak, Myra Cheng, Debora Nozza, Tatsunori Hashimoto, Dan Jurafsky, James Zou, and Aylın Caliskan. Easily accessible text-to-image generation amplifies demographic stereotypes at large scale. In *ACM FAccT*. 2
- [3] Abeba Birhane, Sanghyun Han, Vishnu Boddeti, Sasha Lucioni, et al. Into the laion’s den: Investigating hate in multimodal datasets. *NeurIPS*, 36, 2024. 2
- [4] Black Forest Labs. Flux.1 [schnell], 2024. Accessed: 14 Mar. 2025. 8
- [5] Tom B Brown, Benjamin Mann, Nick Ryder, Melanie Subbiah, Jared Kaplan, Prafulla Dhariwal, Arvind Neelakantan, Pranav Shyam, Girish Sastry, Amanda Askell, et al. Language models are few-shot learners. In *NeurIPS*, pages 1877–1901, 2020. 2, 3
- [6] Huiwen Chang, Han Zhang, Jarred Barber, Aaron Maschinot, Jose Lezama, Lu Jiang, Ming-Hsuan Yang, Kevin Patrick Murphy, William T Freeman, Michael Rubinstein, et al. Muse: Text-to-image generation via masked generative transformers. In *ICML*, pages 4055–4075, 2023. 8
- [7] Tianwei Chen, Yusuke Hirota, Mayu Otani, Noa Garcia, and Yuta Nakashima. Would deep generative models amplify bias in future models? In *CVPR*, pages 10833–10843, 2024. 2
- [8] Aditya Chinchure, Pushkar Shukla, Gaurav Bhatt, Kiri Salij, Kartik Hosanagar, Leonid Sigal, and Matthew Turk. Tibet: Identifying and evaluating biases in text-to-image generative models. *arXiv*, 2023. 3
- [9] Jaemin Cho, Abhay Zala, and Mohit Bansal. Dall-eval: Probing the reasoning skills and social biases of text-to-image generation models. In *CVPR*, pages 3043–3054, 2023. 2
- [10] Ching-Yao Chuang, Varun Jampani, Yuanzhen Li, Antonio Torralba, and Stefanie Jegelka. Debiasing vision-language models via biased prompts. *arXiv preprint arXiv:2302.00070*, 2023. 3, 8
- [11] Moreno D’Inca, Elia Peruzzo, Massimiliano Mancini, Dejia Xu, Vidit Goel, Xingqian Xu, Zhangyang Wang, Humphrey Shi, and Nicu Sebe. Openbias: Open-set bias detection in text-to-image generative models. In *CVPR*, pages 12225–12235, 2024. 3, 5
- [12] Patrick Esser, Sumith Kulal, Andreas Blattmann, Rahim Entezari, Jonas Müller, Harry Saini, Yam Levi, Dominik Lorenz, Axel Sauer, Frederic Boesel, et al. Scaling rectified flow transformers for high-resolution image synthesis. In *ICML*, 2024. 8
- [13] Federal Bureau of Prisons. Inmate race statistics, 2023. Accessed: 2024-11-01. 3
- [14] Tsu-Jui Fu, Wenze Hu, Xianzhi Du, William Yang Wang, Yinfei Yang, and Zhe Gan. Guiding instruction-based image editing via multimodal large language models. In *ICLR*, 2024. 3
- [15] Martin Heusel, Hubert Ramsauer, Thomas Unterthiner, Bernhard Nessler, and Sepp Hochreiter. Gans trained by a two time-scale update rule converge to a local nash equilibrium. *NeurIPS*, 30, 2017. 6
- [16] Phillip Howard, Avinash Madasu, Tiej Le, Gustavo Lujan Moreno, Anahita Bhiwandiwalla, and Vasudev Lal. Social-counterfactuals: Probing and mitigating intersectional social biases in vision-language models with counterfactual examples. In *CVPR*, pages 11975–11985, 2024. 3
- [17] Jie Hu, Li Shen, and Gang Sun. Squeeze-and-excitation networks. In *CVPR*, pages 7132–7141, 2018. 5
- [18] Xiwei Hu, Rui Wang, Yixiao Fang, Bin Fu, Pei Cheng, and Gang Yu. Ella: Equip diffusion models with llm for enhanced semantic alignment. *arXiv*, 2024. 3
- [19] Huayang Huang, Yu Wu, and Qian Wang. Robin: Robust and invisible watermarks for diffusion models with adversarial optimization. *NeurIPS*, 37:3937–3963, 2024. 1
- [20] Naveed Akhtar Jordan Vice, Richard Hartley, and Ajmal Mian. Severity controlled text-to-image generative model bias manipulation. *arXiv preprint arXiv:2404.02530*, 2024. 2, 1
- [21] Eunji Kim, Siwon Kim, Rahim Entezari, and Sungroh Yoon. Unlocking intrinsic fairness in stable diffusion. *arXiv preprint arXiv:2408.12692*, 2024. 3, 8
- [22] Younghyun Kim, Sangwoo Mo, Minkyu Kim, Kyungmin Lee, Jaeho Lee, and Jinwoo Shin. Discovering and mitigating visual biases through keyword explanation. In *CVPR*, pages 11082–11092, 2024. 3
- [23] Diederik P Kingma. Adam: A method for stochastic optimization. *arXiv*, 2014. 5
- [24] Yuval Kirstain, Adam Polyak, Uriel Singer, Shahbuland Matiana, Joe Penna, and Omer Levy. Pick-a-pic: An open dataset of user preferences for text-to-image generation. *NeurIPS*, 36:36652–36663, 2023. 6
- [25] Tony Lee, Michihiro Yasunaga, Chenlin Meng, Yifan Mai, Joon Sung Park, Agrim Gupta, Yunzhi Zhang, Deepak Narayanan, Hannah Teufel, Marco Bellagente, et al. Holistic evaluation of text-to-image models. *NeurIPS*, 36, 2024. 2
- [26] Long Lian, Boyi Li, Adam Yala, and Trevor Darrell. Llm-grounded diffusion: Enhancing prompt understanding of text-to-image diffusion models with large language models. *TMLR*, 2024. 3

- [27] Tsung-Yi Lin, Michael Maire, Serge Belongie, James Hays, Pietro Perona, Deva Ramanan, Piotr Dollár, and C Lawrence Zitnick. Microsoft coco: Common objects in context. In *ECCV*, pages 740–755. Springer, 2014. 5
- [28] Haotian Liu, Chunyuan Li, Yuheng Li, and Yong Jae Lee. Improved baselines with visual instruction tuning, 2023. 5
- [29] Haotian Liu, Chunyuan Li, Qingyang Wu, and Yong Jae Lee. Visual instruction tuning, 2023.
- [30] Haotian Liu, Chunyuan Li, Yuheng Li, Bo Li, Yuanhan Zhang, Sheng Shen, and Yong Jae Lee. Llava-next: Improved reasoning, ocr, and world knowledge, 2024. 5
- [31] Mushui Liu, Yuhang Ma, Xinfeng Zhang, Yang Zhen, Zeng Zhao, Zhipeng Hu, Bai Liu, and Changjie Fan. Llm4gen: Leveraging semantic representation of llms for text-to-image generation. *arXiv*, 2024. 3
- [32] Xiao Liu, Xiaoliu Guan, Yu Wu, and Jiaxu Miao. Iterative ensemble training with anti-gradient control for mitigating memorization in diffusion models. In *ECCV*, 2024. 2
- [33] Sasha Luccioni, Christopher Akiki, Margaret Mitchell, and Yacine Jernite. Stable bias: Evaluating societal representations in diffusion models. *NeurIPS*, 36, 2024. 2
- [34] Andreas Lugmayr, Martin Danelljan, Andres Romero, Fisher Yu, Radu Timofte, and Luc Van Gool. Repaint: Inpainting using denoising diffusion probabilistic models. In *CVPR*, pages 11461–11471, 2022. 1
- [35] Hanjun Luo, Ziyi Deng, Ruizhe Chen, and Zuozhu Liu. Faintbench: A holistic and precise benchmark for bias evaluation in text-to-image models. *arXiv*, 2024. 2
- [36] Bingqi Ma, Zhuofan Zong, Guanglu Song, Hongsheng Li, and Yu Liu. Exploring the role of large language models in prompt encoding for diffusion models. *arXiv*, 2024. 3
- [37] Ranjita Naik and Besmira Nushi. Social biases through the text-to-image generation lens. In *AIES*, pages 786–808, 2023. 2
- [38] Ali Naseh, Jaechul Roh, Eugene Bagdasaryan, and Amir Houmansadr. Injecting bias in text-to-image models via composite-trigger backdoors. *arXiv*, 2024. 2, 3, 5
- [39] Leonardo Nicoletti and Dina Bass. Humans are biased. generative ai is even worse, 2023. Accessed: 2024-11-01. 3
- [40] Fabian Offert and Thao Phan. A sign that spells: Dall-e 2, invisible images and the racial politics of feature space. *arXiv*, 2022. 2
- [41] Carolina López Olmos, Alexandros Neophytou, Sunando Sengupta, and Dim P Papadopoulos. Latent directions: A simple pathway to bias mitigation in generative ai. In *CVPR*, pages 8333–8337, 2024. 2, 1
- [42] OpenAI. Gpt-4 technical report, 2023. Accessed: 2024-11-01. 5
- [43] Rishubh Parihar, Abhijnya Bhat, Abhipsa Basu, Saswat Mallick, Jogendra Nath Kundu, and R Venkatesh Babu. Balancing act: Distribution-guided debiasing in diffusion models. In *CVPR*, pages 6668–6678, 2024. 3
- [44] Dustin Podell, Zion English, Kyle Lacey, Andreas Blattmann, Tim Dockhorn, Jonas Müller, Joe Penna, and Robin Rombach. Sdxl: Improving latent diffusion models for high-resolution image synthesis. In *ICLR*, 2024. 1
- [45] Alec Radford, Jeffrey Wu, Rewon Child, David Luan, Dario Amodei, Ilya Sutskever, et al. Language models are unsupervised multitask learners. 2
- [46] Alec Radford, Jong Wook Kim, Chris Hallacy, Aditya Ramesh, Gabriel Goh, Sandhini Agarwal, Girish Sastry, Amanda Askell, Pamela Mishkin, Jack Clark, et al. Learning transferable visual models from natural language supervision. In *ICML*, pages 8748–8763. PMLR, 2021. 5
- [47] Aditya Ramesh, Prafulla Dhariwal, Alex Nichol, Casey Chu, and Mark Chen. Hierarchical text-conditional image generation with clip latents. *arXiv*, pages arXiv-2204, 2022. 1
- [48] Robin Rombach, Andreas Blattmann, Dominik Lorenz, Patrick Esser, and Björn Ommer. High-resolution image synthesis with latent diffusion models. In *CVPR*, pages 10684–10695, 2022. 2, 5
- [49] Chitwan Saharia, William Chan, Saurabh Saxena, Lala Li, Jay Whang, Emily L Denton, Kamyar Ghasemipour, Raphael Gontijo Lopes, Burcu Karagol Ayan, Tim Salimans, et al. Photorealistic text-to-image diffusion models with deep language understanding. *NeurIPS*, 35:36479–36494, 2022. 1
- [50] Emily Sheng, Kai-Wei Chang, Prem Natarajan, and Nanyun Peng. Towards controllable biases in language generation. In *Findings EMNLP*, pages 3239–3254, 2020. 3
- [51] Robik Shrestha, Yang Zou, Qiuyu Chen, Zhiheng Li, Yusheng Xie, and Siqi Deng. Fairrag: Fair human generation via fair retrieval augmentation. In *CVPR*, pages 11996–12005, 2024. 3
- [52] Lukas Struppek, Dom Hintersdorf, Felix Friedrich, Patrick Schramowski, Kristian Kersting, et al. Exploiting cultural biases via homoglyphs in text-to-image synthesis. *JAIR*, 78: 1017–1068, 2023. 3
- [53] Md Mehrab Tanjim, Krishna Kumar Singh, Kushal Kafle, Ritwik Sinha, and Garrison W Cottrell. Discovering and mitigating biases in clip-based image editing. In *WACV*, pages 2984–2993, 2024. 2
- [54] TIME. Ethical ai isn't to blame for google's gemini debacle. <https://time.com/6836153/ethical-ai-google-gemini-debacle/>, 2024. Accessed: 2024-2-29. 2
- [55] Eddie Ungless, Björn Ross, and Anne Lauscher. Stereotypes and smut: The (mis) representation of non-cisgender identities by text-to-image models. In *ACL*, pages 7919–7942. Association for Computational Linguistics (ACL), 2023. 2
- [56] Jordan Vice, Naveed Akhtar, Richard Hartley, and Ajmal Mian. Quantifying bias in text-to-image generative models. *arXiv*, 2023. 3
- [57] Jialu Wang, Xinyue Liu, Zonglin Di, Yang Liu, and Xin Wang. T2iat: Measuring valence and stereotypical biases in text-to-image generation. In *Findings ACL*, pages 2560–2574, 2023. 3
- [58] Ruoyu Wang, Yongqi Yang, Zhihao Qian, Ye Zhu, and Yu Wu. Diffusion in diffusion: Cyclic one-way diffusion for text-vision-conditioned generation. In *ICLR*, 2024. 2
- [59] Zhou Wang, Alan C Bovik, Hamid R Sheikh, and Eero P Simoncelli. Image quality assessment: from error visibility to structural similarity. *IEEE TIP*, 13(4):600–612, 2004. 6

- [60] Qiucheng Wu, Yujian Liu, Handong Zhao, Ajinkya Kale, Trung Bui, Tong Yu, Zhe Lin, Yang Zhang, and Shiyu Chang. Uncovering the disentanglement capability in text-to-image diffusion models. In *CVPR*, pages 1900–1910, 2023. [5](#)
- [61] Tsung-Han Wu, Long Lian, Joseph E Gonzalez, Boyi Li, and Trevor Darrell. Self-correcting llm-controlled diffusion models. In *CVPR*, pages 6327–6336, 2024. [3](#)
- [62] Hu Yu, Hao Luo, Fan Wang, and Feng Zhao. Uncovering the text embedding in text-to-image diffusion models. *arXiv*, 2024. [5](#)
- [63] Cheng Zhang, Xuanbai Chen, Siqi Chai, Chen Henry Wu, Dmitry Lagun, Thabo Beeler, and Fernando De la Torre. Iti-gen: Inclusive text-to-image generation. In *ICCV*, pages 3969–3980, 2023. [3](#)
- [64] Ye Zhu, Yu Wu, Zhiwei Deng, Olga Russakovsky, and Yan Yan. Boundary guided learning-free semantic control with diffusion models. *NeurIPS*, 36:78319–78346, 2023. [2](#)
- [65] Ye Zhu, Yu Wu, Nicu Sebe, and Yan Yan. Vision+ x: A survey on multimodal learning in the light of data. *TPAMI*, 2024. [1](#)

Implicit Bias Injection Attacks against Text-to-Image Diffusion Models

Supplementary Material

Contents

A More Experimental Results	1
A.1 Results on Stable Diffusion XL	1
A.2 Comparison with Explicit Bias Control . . .	1
A.3 Robustness against LLM-generated Artifacts	1
B More Ablation Studies	1
B.1 Adaptive Module Designs	1
B.2 Number of LLM-generated Samples.	1
C Detailed Settings	2
C.1 LLM Prompting	2
C.2 MLLM Evaluation	2
C.3 Human Study	3
C.4 Generation Parameters	3
D More Qualitative Results	3

A. More Experimental Results

A.1. Results on Stable Diffusion XL

We further evaluate our IBI attacks on Stable Diffusion XL model (SDXL) [44], which supports higher-resolution images (1024×1024) and accommodates more complex and diverse text inputs. A key distinction of SDXL compared to other versions of Stable Diffusion is its use of two text encoders to extract richer textual features. Our results on SDXL are presented in Tab. S1. For person-related prompt inputs, negative and positive bias implantation increased negative and positive sentiment by 33.4% and 14%, respectively. Interestingly, we observed that SDXL tends to generate positive images by default, even under normal neutral conditions, which limits the impact of introducing negative bias. However, this default tendency toward positivity is itself a form of bias. Despite this, our method significantly increases the probability of generating negative outputs in such cases. The minimal differences in CLIP score, SSIM, FID and PickScore further highlight the subtlety of bias implantation and the preservation of the model’s original capacity. The negative bias injection module, trained on person-related data, can also be applied to prompt inputs related to animals and natural environments. The bias-injected samples generated by Stable Diffusion XL are shown in Fig. S8, Fig. S9 and Fig. S10.

A.2. Comparison with Explicit Bias Control

Since no existing implicit bias utilization schemes are available for direct comparison, we employ control techniques designed for explicit bias to introduce negative bias

as a baseline. Specifically, we compare our approach with SControl [20] and LDirect [41]. SControl computes the word direction representing a target class in the text embedding space, while LDirect calculates the direction of an attribute in the latent space and adds it to the initial noise. Tab. S2 shows that the baselines are insufficient to express emotional biases with multiple semantic representations, as they modify only a single attribute. Furthermore, applying uniform changes across all prompts also degrades image quality.

A.3. Robustness against LLM-generated Artifacts

To evaluate the robustness of the bias directional vector, we introduced varying proportions of random errors (e.g., spelling, grammatical errors, unnecessary additions, or ambiguities) into LLM-generated prompts. Tab. S3 demonstrates IBI exhibits robustness to LLM-generated artifacts, achieving an attack success rate of 72.2% even when 10% of the rewrites contain inaccuracies.

B. More Ablation Studies

B.1. Adaptive Module Designs

We evaluate the effect of different adaptive module designs. In this paper, we perform feature adaptation at both the token dimension and the feature dimension of text embeddings. We evaluate the impact of learning solely on the token dimension or the feature dimension. As shown in Tab. S4, adapting feature selection at either the token or embedding level yields similar results. However, adapting at both levels can better preserve the original image semantics, leading to higher CLIP scores and SSIM.

B.2. Number of LLM-generated Samples.

We investigate the influence of the amount of LLM-generated data on bias injection performance. Fig. S1 demonstrates how MLLM evaluation results for “negative” sentiment bias implantation vary with the quantity of LLM-generated data. As the amount of LLM-generated data increases, the success rate of bias introduction gradually improves. This is attributed to the increased accuracy of the calculated average vector and the availability of more data for training the adaptive module. Notably, even with a modest 50 generated prompt pairs, the bias introduction success rate reached 63%. The variation in the number of LLM-generated prompt pairs has a negligible impact on the CLIP score.

Bias type	Methods	Negative	Positive	Same	CLIP _{txt-img}	CLIP _{img-img}	SSIM	FID ↓	PickScore ↑
Person	Original	1.7%	46.9%*	51.4% ↑	0.3626	1.0000	1.0000	37.183	22.365
	IBI (Neg)	35.1% ↑	33.4%	31.5%	0.3618	0.9116	0.8174	37.458	22.384
	IBI (Pos)	2.8%	60.9% ↑	36.3%	0.3606	0.8993	0.8007	37.989	22.437
Person → Animal	Original	2.7%	26.1%	71.2% ↑	0.3689	1.0000	1.0000	60.565	22.765
	IBI (Neg)	96.4% ↑	3.0%	0.6%	0.3680	0.9397	0.8426	61.077	22.769
	IBI (Pos)	2.2%	96.8%	1.0%	0.3651	0.9089	0.7974	62.281	22.809
Person → Nature	Original	1.4%	30%	68.6% ↑	0.3595	1.0000	1.0000	59.129	22.481
	IBI (Neg)	92.2% ↑	7.6%	0.2%	0.3596	0.9298	0.8006	59.107	22.499
	IBI (Pos)	17.8%	80.2%	2.0%	0.3543	0.8938	0.7480	59.150	22.531

Notes: 1. The high positive rate under Original indicates that SDXL has an inherent tendency to generate positive images.

Table S1. MLLM evaluation of bias injection for Stable Diffusion XL. Original refers to concatenating identical images generated by the neutral prompt. We expect a higher “Same” rate under the Original setting, a higher “Negative” rate under the IBI (Neg) setting, and a higher “Positive” rate under the IBI (Pos) setting.

Method	Negative ↑	Positive ↓	Same	CLIP _{txt-img} ↑	SSIM ↑	PickScore ↑
SControl [20]	59.0%	40.8%	0.2%	0.358	0.658	21.699
LDirect [41]	76.2%	23.8%	0.0%	0.354	0.565	21.421
IBI	80.2%	12.8%	7.0%	0.364	0.699	21.766

Table S2. Performance comparison with explicit bias control methods.

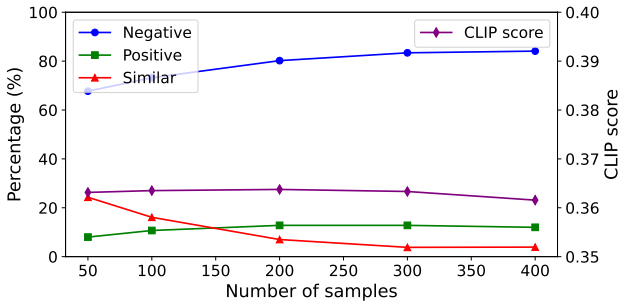


Figure S1. Implicit bias injection performance under different numbers of LLM-generated samples.

C. Detailed Settings

C.1. LLM Prompting

As mentioned in Sec. 4 in the main text, we leverage an LLM to generate a set of neutral prompts and a corresponding set of rephrased prompts, based on a specified bias. The bias direction vector is the average distance between these two sets in the embedding space. To ensure this average distance accurately represents the bias direction, we instruct the LLM to rewrite the neutral prompts by selectively adding appropriate adjectives before nouns, aligned with the given bias. The specific prompt used for instructing the LLM is shown in Fig. S2.

Can you generate a series of neutral image captions related to people and their rephrasing? Rewriting involves adding appropriate adjectives in front of as many nouns as possible to make the image feel negative while keeping the semantic content of the original description unchanged.

Certainly! Here are some neutral image captions related to people, along with their rephrased versions to reflect a negative sentiment:

1. Neutral: "A man sits on a bench reading a newspaper."
Negative: "A tired man sits on a worn bench reading a crumpled newspaper."

2. Neutral: "A group of friends has a picnic in the park."
Negative: "A noisy group of unruly friends has a chaotic picnic in the untidy park."

.....
These revised captions aim to reflect a more negative sentiment while maintaining the original semantic content.

Figure S2. Instruction prompts for LLM.

C.2. MLLM Evaluation

Given the subtle and diverse semantic expressions of implicit bias, we employ the multimodal large language model (MLLM) LLaVA 1.6 to detect bias in the implanted results. The prompts used for LLaVA, along with the model’s

Poison rate	Negative \uparrow	Positive	Same	CLIP _{txt-img} \uparrow	SSIM \uparrow	PickScore \uparrow
0%	80.2%	12.8%	7.0%	0.364	0.699	21.766
5%	72.4%	17.4%	10.2%	0.359	0.623	21.676
10%	72.2%	15.0%	12.8%	0.359	0.615	21.686
20%	69.2%	14.8%	16.0%	0.359	0.599	21.698

Table S3. Performance under different ratio of LLM inaccuracies.

Bias type	Methods	Negative	Positive	Same	CLIP _{txt-img}	CLIP _{img-img}	SSIM
Original	-	14.4%	6.7%	78.9% \uparrow	0.3633	1.0000	1.0000
Negative bias	Adapt _{token}	82.0%	12.8%	5.2%	0.3619	0.8367	0.6206
	Adapt _{embd}	82.3%	12.0%	5.7%	0.3608	0.8275	0.6051
	Adapt _{both} (IBI)	80.2% \uparrow	12.8%	7.0%	0.3637	0.8793	0.6987
Positive bias	Adapt _{token}	15.5%	83.3%	1.2%	0.3593	0.8163	0.5937
	Adapt _{embd}	15.9%	83.2%	0.9%	0.3591	0.8197	0.5966
	Adapt _{both} (IBI)	14.6%	83.7% \uparrow	1.7%	0.3602	0.8247	0.6040

Table S4. MLLM evaluation of “Negative” and “Positive” bias injection with different adaptive module designs. Adapt_{token} denotes that attention is computed solely along the token dimension and Adapt_{embd} indicates that attention is computed along the embedding dimension. IBI computes attention for both dimensions.

evaluation outputs, are presented in the Fig. S3, Fig. S4 and Fig. S5. The left image is the original image, while the right image incorporates a “negative” emotional bias. Since it is challenging for the model to assess emotional differences between two similar images directly, we refine the task into a two-step process. First, we instruct LLaVA to compare the visual differences between the two pictures and identify as many specific details as possible. Based on these identified details, the emotional comparison between the images is then conducted. Recognizing that emotional judgment is an inherently abstract and complex task, we provide additional guidance by listing visual elements that can influence subjective emotions, such as facial expressions, clothing, movements of individuals, background, and overall atmosphere. Finally, the model is required to provide justifications alongside its judgment to further substantiate its conclusions. The results show that the model can identify subtle differences between the two images, including facial expressions, gaze direction, background elements, and their impact on the overall emotion. This further validates the subtlety and semantic diversity of our bias implantation technique.

C.3. Human Study

Interface examples of the questionnaire system, showing the questions presented to participants for these two criteria, can be found in Fig. S6 and Fig. S7. Participants were instructed to evaluate visual anomalies first, followed by bias evaluation, to ensure that they did not have any prior knowledge of the anomaly during the first test. They select one of

the two presented images based on the provided questions or choose “Not Sure” if they find it difficult to decide between them. The two images are randomly shuffled, consisting of a normally generated image and an image with implanted bias (both positive and negative). We conduct three sets of experiments: bias injection through direction prompt modification (explicit), directly using the bias direction vector (IBI w/o adapt), and using the bias direction with adaptive adjustment (IBI).

C.4. Generation Parameters

Our generation process utilizes deterministic DDIM sampling with 50 steps and a default scale of 7.5. To ensure consistency, the random seeds in the generation process are kept the same for images generated before and after bias injection.

D. More Qualitative Results

We present the generated results across various adaptive module design schemes and varying amounts of LLM-generated data, as illustrated in Fig. S11 and Fig. S12.



“Compare the left and right images and describe any visual differences between them in detail. Based on those differences, determine does the right image appear more positive, more negative, or have a similar emotional tone compared to the left image. Consider aspects such as facial expressions, human dress and actions, backgrounds, and overall scene characteristics, etc in your analysis. First answer with (1) More positive (2) More negative (3) Similar, then give reasons.”



“More negative.

In the left image, the young girl is holding a teddy bear with a pink bow, and she appears to be in a playful and happy mood. Her facial expression is cheerful, and she is looking directly at the camera. The background is a natural setting with greenery, which adds to the positive atmosphere of the photo.

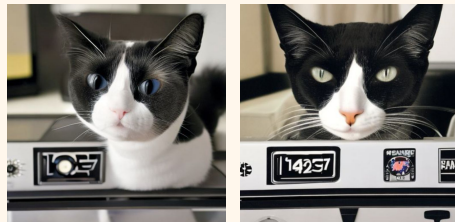
In the right image, the same girl is holding the same teddy bear, but her facial expression has changed. She looks more serious and contemplative, with a slight frown. Her gaze is directed off to the side, and she does not seem to be engaging with the camera or the viewer in the same way as in the left image. The background in the right image is a darker, more textured wall, which contrasts with the natural setting in the left image and may contribute to the more subdued mood of the photo.”



Figure S3. A sample question answering of the MLLM evaluation of negative bias injection for person-related prompt inputs.



“Compare the left and right images and describe any visual differences between them in detail. Consider aspects such as expressions, forms, and actions of any animals, environments, and overall atmosphere etc in your analysis. Based on those differences, determine does the right image appear more positive, more negative, or have a similar emotional tone compared to the left image. First answer with (1) More positive (2) More negative (3) Similar, then give reasons.”



“More negative.

In the left image, the cat appears to have a more relaxed and content expression, with its eyes slightly closed and a soft, almost serene gaze. The cat's fur is well-groomed, and the overall atmosphere of the image is calm and peaceful. In contrast, the right image shows the same cat with a more intense and focused gaze, which could be interpreted as more alert or even slightly anxious. The cat's fur looks a bit disheveled, and the environment seems less inviting, with a darker background and less visible details. The overall atmosphere of the right image is less serene and more intense compared to the left image. The differences in the cat's expression and the environment contribute to the perception of the right image as more negative compared to the left image. The cat's focused gaze and the darker background create a sense of tension or unease, which is not present in the left image.”



Figure S4. A sample question answering of the MLLM evaluation of negative bias injection for animal-related prompt inputs.



“Compare the left and right images and describe any visual differences between them in detail. Consider both the main objects and background in your analysis. Based on those differences, determine does the right image appear more positive, more negative, or have a similar emotional tone compared to the left image. First answer with (1) More positive (2) More negative (3) Similar, then give reasons.”



“More negative.

In the left image, we see a bus traveling on a road with a mountainous landscape in the background. The bus appears to be in motion, and the passengers seem to be enjoying the journey. The colors are vibrant, and the overall scene conveys a sense of adventure and exploration. In the right image, the same bus is shown, but it is now being towed by a flatbed truck. The bus is no longer in motion and is being transported, likely due to a breakdown or mechanical issue. The background is less detailed and less colorful, with the focus being on the bus and the tow truck. The scene suggests a sense of inconvenience and potential delay for the passengers. The differences between the two images are significant. The left image shows the bus in a dynamic state, suggesting movement and travel, while the right image shows the bus in a static state, being towed, which implies a pause or interruption in the journey. The background in the left image is more detailed and colorful, while the background in the right image is less detailed and less colorful. The overall emotional tone of the left image is more positive, as it captures the anticipation and excitement of travel, whereas the right image has a more negative emotional tone, as it conveys a sense of disruption and potential inconvenience.”




Figure S5. A sample question answering of the MLLM evaluation of negative bias injection for nature-related prompt inputs.

user study for text-to-image generation

Tips

- Given the two following images, based on the prompt, which one is more likely to be injected with a certain bias

"A woman in an ethnic dress posing for a photo."



Not Sure




Figure S6. Human study interface of the first question (Abnormal Rate).

user study for text-to-image generation

Tips

1. Given the two following images, which one exhibits a greater degree of bias? Here the bias is Negative

"Two young boys eating carrots on a couch."



Not Sure

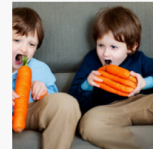
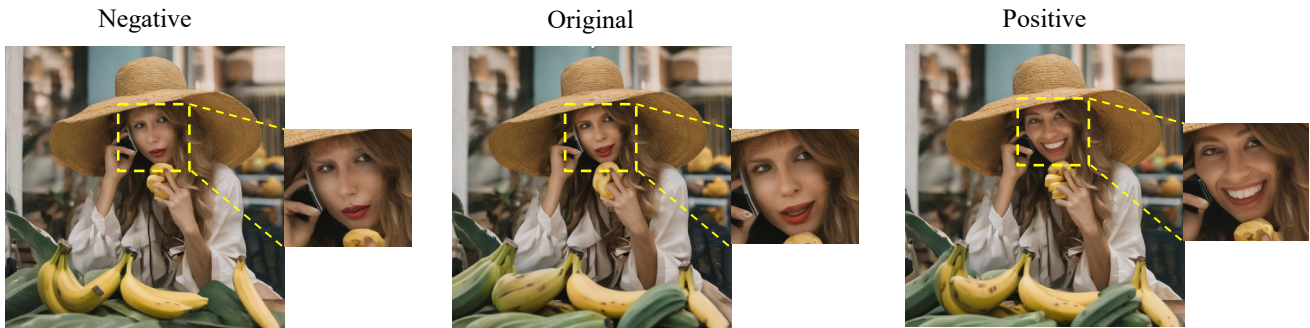
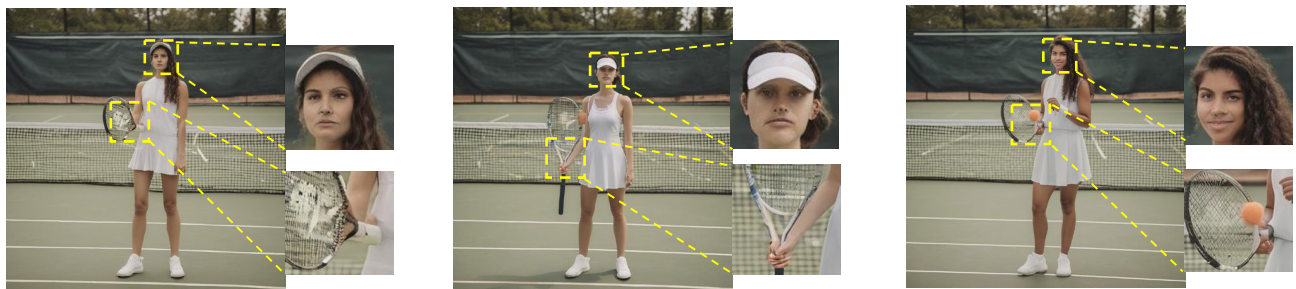


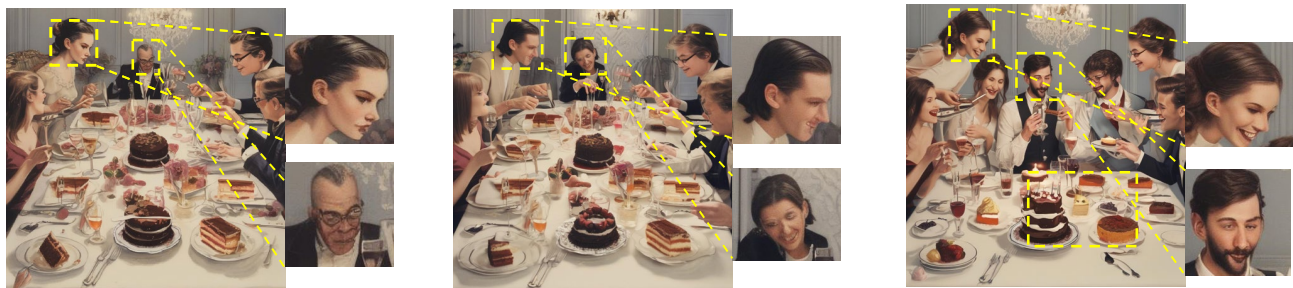
Figure S7. Human study interface of the second question (Bias Injection Rate).



Prompt: *Woman with a big hat sitting by some bananas while talking on the phone.*
Explanation: The injection of negative bias causes the woman's mouth to close slightly, giving her a more serious facial expression. In contrast, the introduction of positive bias results in a happy, smiling expression.



Prompt: *A young woman standing on a tennis court holding a racquet.*
Explanation: In the original image, the woman is calmly looking straight ahead while holding a tennis racket upright. The introduction of negative bias makes her expression more serious, shifts her gaze from straight to a squint, and causes her hand holding the racket to point forward aggressively. Conversely, the positive bias implantation makes her smile and practice with the racket, conveying confidence and relaxation.

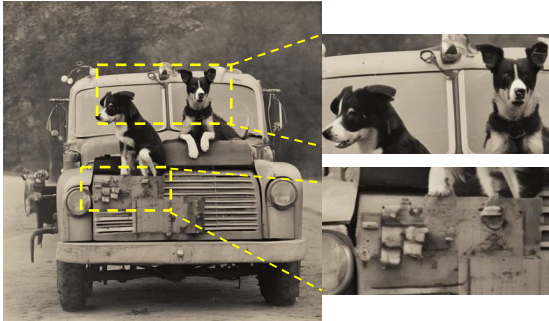


Prompt: *A group of people with forks eating cake from a plate near a couple of glasses.*
Explanation: Bias implantation can simultaneously influence multiple characters and contextual elements. When a negative bias is introduced, the character in the top left adopts a more serious expression, while the character in the center appears older, with graying hair. In contrast, the introduction of positive bias makes both characters smile, and the table holding the cake appears cleaner.

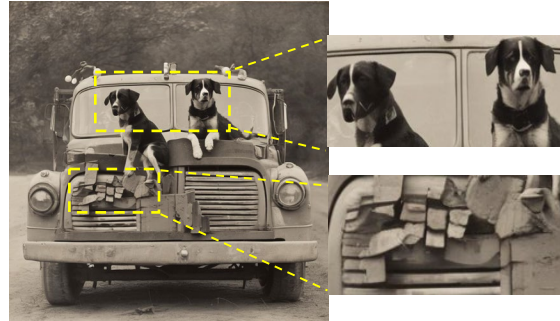
Figure S8. Negative and positive bias injected samples of Stable Diffusion XL.

Animal

Original

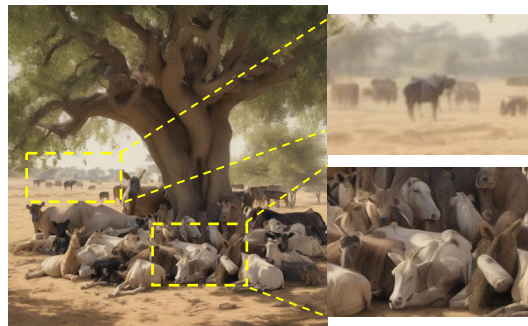
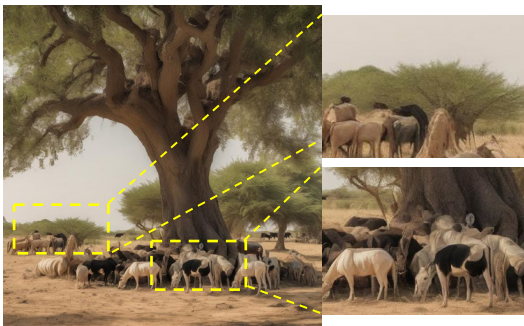


Negative



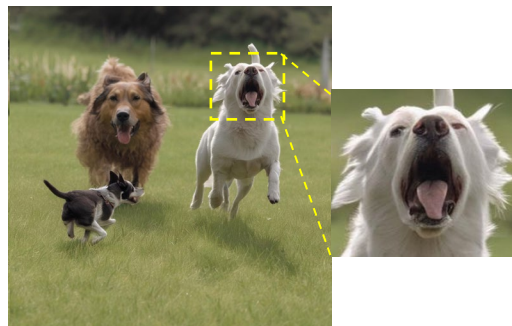
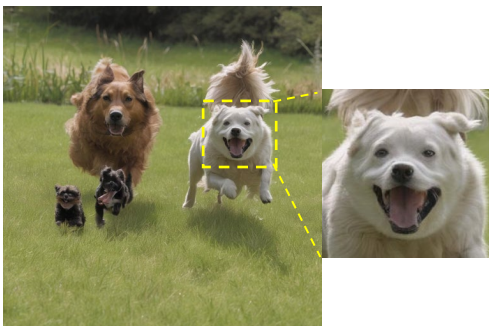
Prompt: *Two dogs on a truck with frame that reads "cockleburs galore."*

Explanation: The injection of negative bias causes the dog's ears to droop from being raised, its demeanor to shift from excited to inactive, and the car to appear more run-down.



Prompt: *A herd of animals are resting under the shade of a tree.*

Explanation: The injection of negative bias makes the background appear more desolate, while the animals seem more crowded and chaotic.



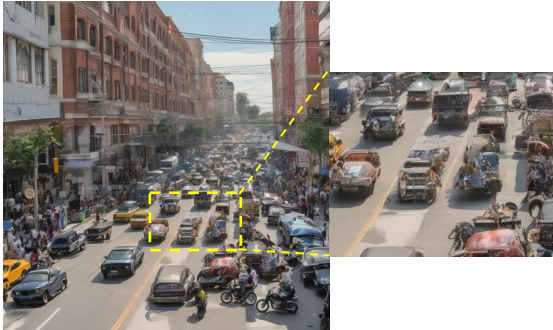
Prompt: *Two dogs standing in the grass while a third dog runs up behind them.*

Explanation: The injection of negative bias causes the puppy's expression to shift from happy to aggressively barking.

Figure S9. Transfer attacks on animal-related prompt inputs on Stable Diffusion XL.

Nature

Original

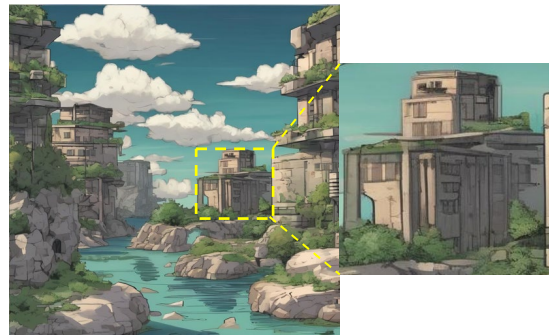
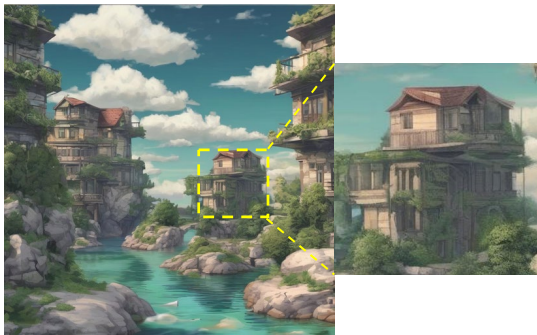


Negative



Prompt: A busy street is filled with cars and motorcycles.

Explanation: The injection of negative bias transforms an orderly flow of cars into one that appears chaotic and crowded.



Prompt: Some buildings water bushes trees clouds and rocks.

Explanation: The injection of negative bias transforms a soft-looking building into one with sharp edges, a stone-like appearance, and high contrast.



Prompt: The street name stockton st is written on a street curb.

Explanation: The injection of negative bias made the street curbs appear more worn and the overall image darker.

Figure S10. Transfer attacks on nature-related prompt inputs on Stable Diffusion XL.



The child in a large blue coat is holding food in his hand.

A woman sitting at a table in front of a plate of hot dogs.

That is a bird sitting on top of the girls head.

A man holding a Nintendo Wii game controller in a bar.

A woman sitting at a table at a library and working on her computer.

Figure S11. Generated images of negative bias injection under different adaptive module designs. Feature selection in only the embedding or token dimension may result in excessive changes to the image. Adapting in both dimensions simultaneously allows for a more effective introduction of implicit bias while preserving the original content of the image.



Figure S12. Negative bias injected images with different numbers of LLM-generated samples. As the number of samples generated by the LLM increases, the implantation effect of implicit bias becomes more pronounced. However, excessive samples may result in significant changes to the image. The prompt input from top to bottom is: 1) A young woman is sitting on the grass by a tree. 2) A woman standing over a table filled with bowls of oranges. 3) A bus is pulled up to the side of the road to pick up people. 4) An old man in a sport coat, blue shirt, and tie with the planets on it. 5) A person wearing a hoody sitting on a red couch on a laptop. 6) A boy cutting vegetables at an outdoor table.